International Conference
Nuclear Energy for New Europe 2008
Portorož / Slovenia / September 8-11
http://www.djs.si/port2008

Post-Test Analysis of the QUENCH-13 Experiment

Jon Birchley[1], Henrique Austregesilo[2], Christine Bals[2], Roland Dubourg[3], Tim Haste[1], Jean-Sylvestre Lamy[4], Terttaliisa Lind[1], Bernard Maliverney[4], Catherine Marchetto[3], Anna Pinter[5], Martin Steinbrück[6], Juri Stuckert[6], Klaus Trambauer[2]

[1] Paul Scherrer Institut (PSI), CH-5232 Villigen PSI, Switzerland
[2]Gesellschaft für Anlagen und Reaktorsicherheit Forschungsinstitute (GRS), D-85748 Garching bei München, Germany
[3] Institut de Radioprotection et de Sûreté Nucléaire (IRSN), Bât. 702 – BP 3, F-13115 St Paul Lez Durance Cedex, France
[4] Electricité de France R&D (EDF), 1 Avenue Général de Gaulle, F-92141 Clamart,
[5]Atomic Energy Research Institute, H-1525 Budapest, Hungary
[6] Forschungszentrum Karlsruhe (FZK), Hermann-von-Helmholtz-Platz 1, D-76344 Eggenstein-Leopoldshafen, Germany
jonathan.birchley@psi.ch, tim.haste@psi.ch

ABSTRACT

The QUENCH experimental programme at Forschungszentrum Karlsruhe investigates phenomena associated with reflood of a degrading core under postulated severe accident conditions, but where the geometry is still mainly rod-like and degradation is still at an early phase. The latest experiment, QUENCH-13, is the first in this programme to include a silver/indium/cadmium (SIC) control rod of prototypic PWR design. The effects of the control rod on degradation and reflood behaviour are examined under integral conditions, and for the first time the release of SIC aerosols following control rod rupture is measured. These materials can affect the chemistry of fission products in the reactor circuit, and hence the radioactive source term to the environment in the event of containment failure. In particular, the sharp release of cadmium on control rod failure, up to tens of percent of the inventory, was previously ill-defined experimentally. Pre-test calculations to define the test protocol were coordinated through the Source Term area of the EU 6th Framework Network of Excellence SARNET, linking the experimental team at FZK with modellers at PSI, GRS and EDF. FZK are also performing separate-effects tests on small PWR control rod segments, that helped to define the test conditions, and are assisting in understanding the results.

QUENCH-13 was successfully performed according to the agreed specification in November 2007. Failure of the control rod with melt release and first aerosol detection was observed at about 1415 K, while significant release was observed at 1450 K, with indication of massive melt relocation at 1500 K on the control rod. The test was terminated by reflood with cold water at 1813K, following further degradation of the bundle. Large amounts of data were obtained on the thermal response of the bundle, hydrogen production, melt relocation in the bundle, and on SIC aerosol release (total rate, and composition at specific times).

The results are being analysed on the same collaborative basis, using the major severe accident codes SCDAP/RELAP5 (S/R5), ATHLET-CD, MAAP4 and ASTEC. The paper presents the main results of the experiment along with conclusions so far of the post-test calculations regarding the adequacy of the modelling in these codes, and regarding the implications for plant sequence calculations.

1. INTRODUCTION

Release of absorber material following failure of the Silver-Indium-Cadmium (SIC) control rods during a PWR reactor accident can have a strong bearing on the transport in the Reactor Coolant System (RCS) and chemical form of fission products transported to the containment. Relocation of liquefied SIC within the fuel bundle can also impact the degradation of nearby rods and possibly other aspects of the in-core behaviour as well. There is currently a wide uncertainty concerning these processes and consequently no validated modelling treatment is available in any of the reactor analysis codes. The current knowledge is essentially encapsulated in the reviews by Petti [1,2]. Recent and ongoing efforts to redress the knowledge limitations are being pursued within the current SARNET programme, and are summarised by Dubourg et al [3]. The subject of the present paper is the QUENCH-13 experiment [4] which was performed as part of this collective effort. The support to QUENCH-13 comprised coordinated pre-test analyses by PSI, GRS and EDF. In addition, complementary separate effects tests on small control rod samples were conducted by FZK [5] in order to characterise the failure mode and conditions. The test definition and results are summarised in section 2. Post-test analyses to date are briefly described in section 3, and tentative conclusions presented in section 4.

2. SUMMARY OF QUENCH-13

The QUENCH facility is constructed to investigate the hydrogen source term resulting from water injection into an uncovered core of a Light Water Reactor as well as the high-temperature behaviour of core materials under transient conditions.

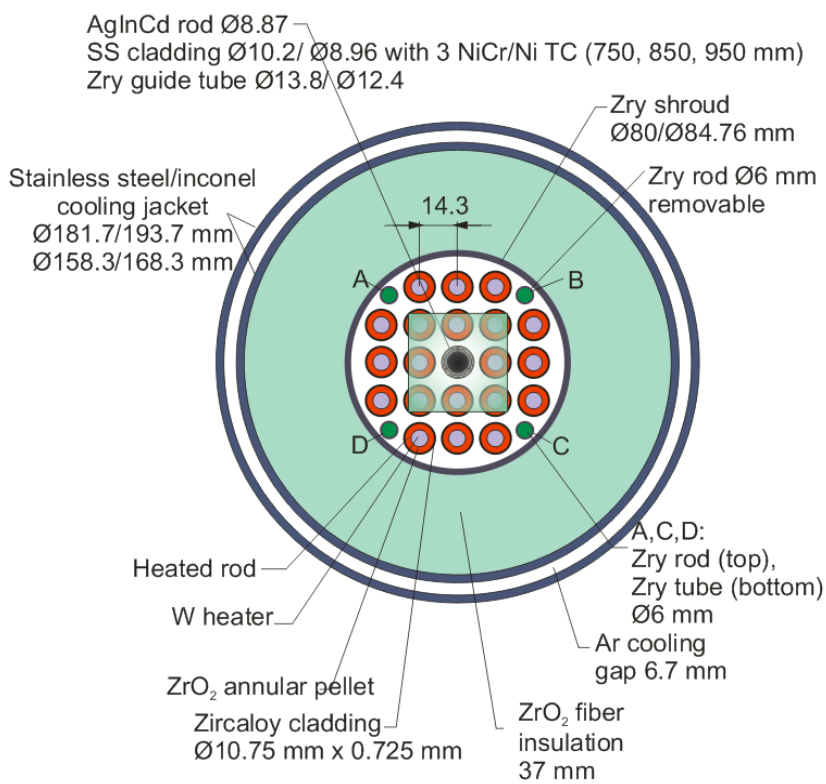

Figure 1: Cross-section of QUENCH-13 test bundle

The QUENCH-13 test bundle consists of 20 fuel rod simulators and one centrally located SIC control rod, and is of total length of approximately 2.5 m (Figure 1). The heating is electric with 1 m length tungsten heaters inside the fuel rod simulators which have standard Zircaloy-4 cladding. The fuel is represented by the ZrO_2 pellets. During the test, some of corner rods, inserted in the bundle to monitor the gas channel conditions could be withdrawn. The bundle is extensively instrumented with about 60 thermocouples distributed along 17 axial positions. The test comprised pre-oxidation at temperature below the rod rupture, then slow ramp temperature transient defined for accurate observations around the rod rupture, and at last, quench water injection at the bottom of the test section (Figure 2). Sampling and on-line measurements of aerosols were performed by PSI and AEKI. Pre-test planning support and preliminary post-test analyses was performed by PSI, GRS and EDF using computer codes S/R5, ATHLET-CD and MAAP, respectively. Post-test calculations have been performed also by IRSN, using the ASTEC code.

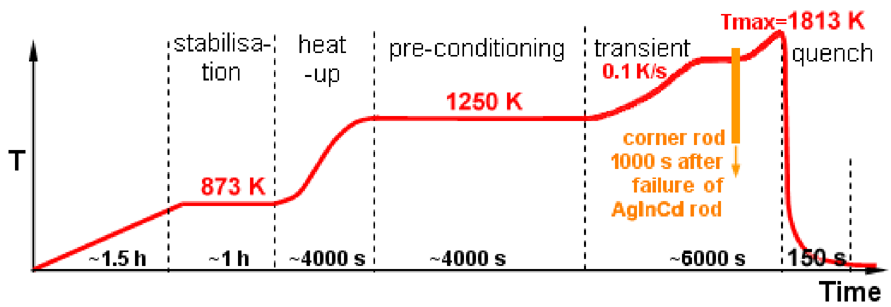

Figure 2: Schematic of QUENCH-13 test conduct (temperature profile on hottest elevation of 950 mm).

The control rod temperature and transported aerosol traces are shown in Figure 3. The first indication of possible control rod damage was a sudden reduction of absorber temperature from about 1400 K at about 10000 s. A positive indication of control rod failure was additionally given by the on-line aerosol monitoring system (electrical low-pressure impactor), which showed a sudden increase in count rate at about 10850 s. A second, much larger aerosol peak, of short duration, was observed at 11500 s, followed by a sustained period of aerosol release that continued until the sampling system was isolated just before reflood. It was confirmed by metallographic examinations [5] that failure occurred at the 950 mm elevation.

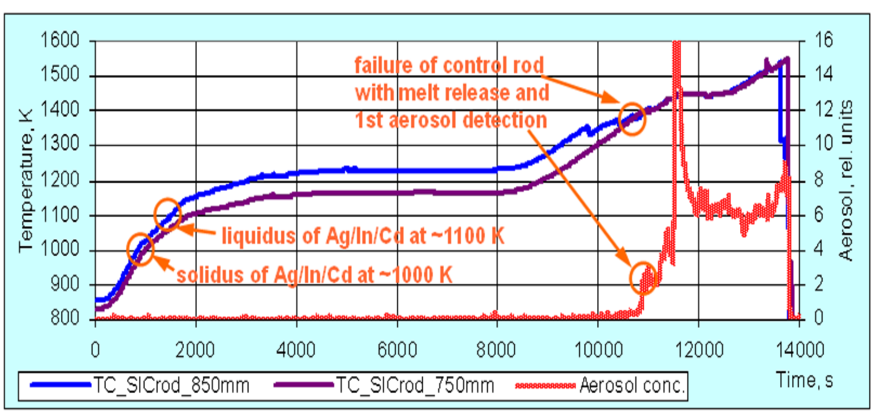

Figure 3: QUENCH-13 sequence of events

Tables 1 and 2 show the composition of aerosols sampled by PSI and AEKI, respectively. It should be noted that the samples reflect aerosols transported through the off-gas line; some unknown fraction of the released material, possibly dependent on composition and particle size, may have been deposited upstream. A total of about 12 g of transported aerosols is estimated from the continuous on-line measurements. The aerosol measurements show a bimodal size distribution suggesting two release modes: vaporisation of volatile species which nucleate and condense forming sub-micron particles, and entrainment by the evolving vapour of liquid droplets of several microns in size. The fine particle mode formed from vaporized species contained approximately 4.5 g of the total of 12 g aerosol mass measured.

Sample	Time (s)	Cd	In	Ag	W	Fe
PSI BI1	12118	42	41	2.5	14.5	
PSI BI3	13692	33	31	8	27	1

Table 1: Elemental composition of aerosols released after CR failure (BI1) and before reflood (BI3); wt%

The impactor sample taken by AEKI just after the first indication of failure showed only Cd, while both sets of samples indicated mainly Cd and In during the initial major release and an increasing fraction of Ag in the later sample, taken when the bundle temperatures were higher.

Sample	O	Cd	In	W	Ag	Zr	Sn	Fe	Mo
AEKI I3	34	55.3	0	0	0	0	0	0	0
AEKI Ni	30.9	15	14.7	9.4	0.7	18.3	4.9	1.7	3.1

Table 2: Selected AEKI aerosol sample data; wt%.

A very approximate indication of the masses of transported Ag, In and Cd can be deduced from the on-line measurements together with the mass composition of the PSI and AEKI samples: Ag 0.5 – 2.5 g (0.1 - 0.5%), In 2 – 5 g (1.5 – 4%), Cd 3 – 6 g (10-20 %).

The material interaction and damage processes in the control rod appeared to limit the locally observed temperatures. Higher temperatures, up to about 1800 K were observed on the shroud and heater rods just at the time of reflood initiation. However, a temporary cooling phase was observed at some fuel rod locations after the large release of absorber material. A total of 42 g of hydrogen was generated, with no significant oxidation or heatup during reflood. Melting was limited to the release and relocation of SIC and its interaction with fuel rod cladding, thus achieving the objective of concentrate on these impacts on degradation. Post-test endoscopic investigation of bundle structures revealed the presence of relocated melt at elevations between third and first spacer grids (550 mm down to 100 below the main heated section).

	Ag	In	Cd	Zr	Fe	Cr	Ni	O	area (%)
1	87	4	8	1					20
2	39	12	0.5	45	3		0.4		79.5
3	10	4	1	37	28	11	1	8	0.5

Table 3: Composition (wt%) of frozen melt at 550 mm.

The cross-section at 550 mm shows an inhomogeneous melt composition (table 3), in which most of the melt comprised roughly equal amounts of SIC and Zircaloy from the guide tube, with a smaller fraction almost entirely SIC and a very small amount of solidified SIC-steel-Zircaloy. The contrasting compositions are visible in figure 4 and suggest possibly different interaction pathways. However, the cross section at this elevation might not be typical of the entire melted mass.

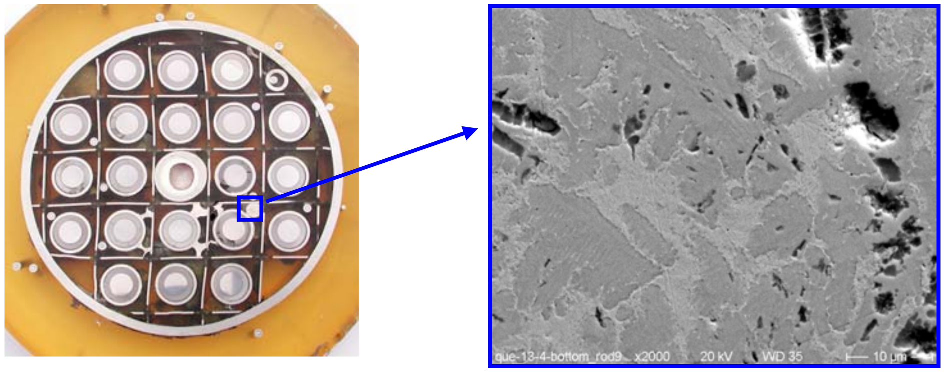

Figure 4: Bundle cross-section (L) at elevation 550 mm. and structure of frozen melt (R)

3. SUMMARY OF POST-TEST ANALYSES

The codes and input models used in the analyses of QUENCH-13 possess contrasting strengths and limitations and the various simulations have concentrated on the different features of the experiment. S/R5 provides a detailed description of the thermal-hydraulics and early phase degradation, including a dynamic model for control rod failure. It is comprehensively benchmarked against QUENCH and has been used in pre- and post-test analyses throughout the programme. MAAP provides a complete description of a whole nuclear plant but adopts a simplified treatment of the in-core processes. The following summary of calculations thus covers all of the QUENCH-13 features in a rather piecewise manner, reflecting the above remarks. The S/R5, MAAP and ATHLET post-test calculations followed on from the pre-test analyses, in which the input models were the starting point and modified according to the actual test conduct.

3.1 S/R5 analysis of bundle behaviour.

The S/R5 analysis concentrated on the bundle thermal response, the hydrogen generation, the control rod degradation and the reflood. The base case calculation correctly followed the evolution until control rod failure. SCDAP uses a mechanistic model to calculate the interaction between the stainless steel cladding and the Zircaloy guide tube, and reproduced the time and temperature of this event with fair accuracy. It should be noted that the sample tests demonstrated a range of failure modes and temperatures, indicating an inherent uncertainty in any predictive method. The SIC relocation was qualitatively captured but the versions available currently do not include aerosol release and transport, nor any treatment of interaction between molten SIC and other materials. The calculation did not capture the unexpected temporary decrease in both the temperatures at the hot elevation and in the hydrogen generation rate following control rod failure, and so calculated the final escalation to occur earlier than observed.

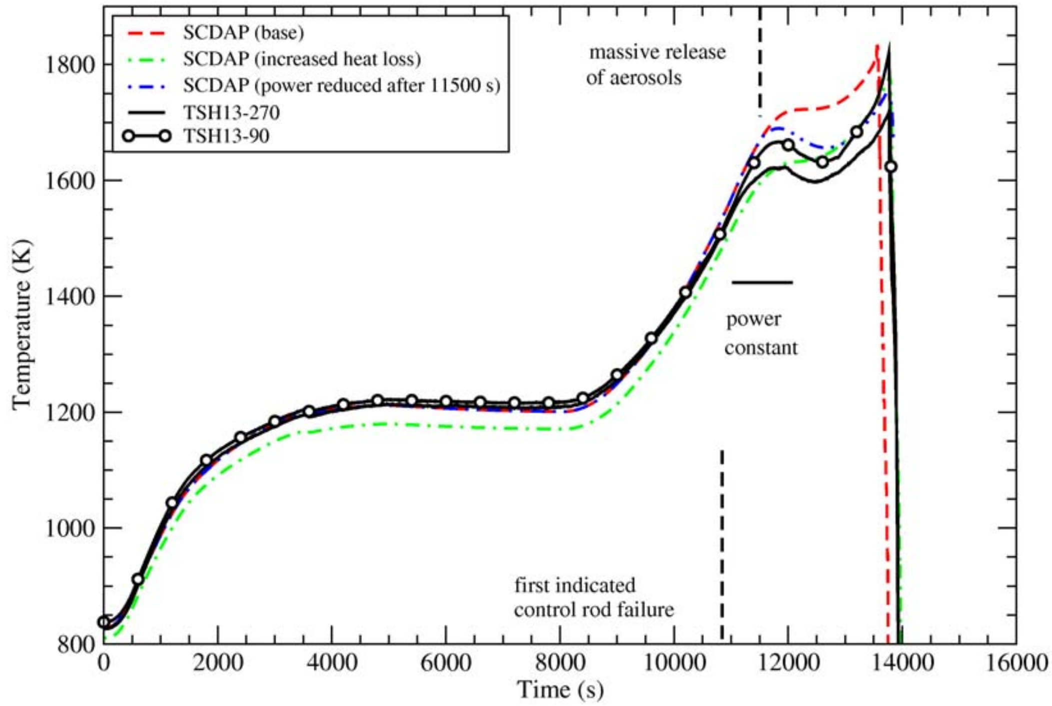

Figure 5: QUENCH 13 experimental data and calculated shroud temperature at 950 mm (SCDAP)

Sensitivity calculations with S/R5 indicate that the cause of the unexpected behaviour was reduced oxidation rate. It is conjectured that the released SIC impinged onto the nearby cladding temporarily inhibited the oxidation. The temperatures are compared in figure 5. There were slight differences between the results but they all calculated control rod failure at a similar temperature and time to those observed and about 40 g of hydrogen generated. All the cases showed similar control rod degradation. Melting was calculated to occur at elevations from 600 mm to the top with relocation to the 100 to 300 mm elevation. Comparison of the extent and mass of relocated material is not yet possible, awaiting further examinations of the bundle. The main signatures are summarised in table 4.

	Base (pre-test + Q-13 boundary conditions)	Increased heat loss	Reduced power (500 W) after 11500 s	Q-13 data
Control rod failure time (s)	10250	10480	10250	10840
Control rod failure temperature (K)	1434	1435	1434	ca. 1415*
Mass of SIC relocated (g) - from elevation (mm) - to elevation (mm)	257 600 to 1024 100 to 300	257 600 to 1024 100 to 300	257 600 to 1024 100 to 300	 -150 to 550
Mass of H2 generated (g)	42	37	40	42
Quench initiation on - time (s) - peak shroud temperature (K)	temperature (13545) 1819	time 13763 (1774)	time 13763 (1814)	temperature 13766 1819

Table 4: QUENCH-13 experiment and calculated signatures

3.2 ASTEC, ATHLET and MAAP analysis of SIC aerosol release

Post-test calculations using ASTEC (V2dev version) correctly reproduced the bundle temperature history at the different levels. At present no mechanistic models are available in the code for accurate reproduction of the control rod modes of rupture. A user defined criterion is used for this rupture, in the present case based on the stainless steel melting temperature of 1723K. This is effectively an upper bound which significantly overestimates the time of rupture, indicating that an appropriate model for Fe-Zr interaction (or at least a user-defined criterion based on temperatures deduced from separate-effects tests) is needed.

The instantaneous released masses of absorber materials calculated by the ASTEC code are given in figure 6. A superficial comparison shows that the code reproduces the main trends for Cd and In, in particular the observed aerosol composition (mainly Cd and In), just after the rod rupture and during the main aerosol release (see figure 3 and table 2). The figure 7 shows the mass fractions, defined as the ratio between the cumulated released mass and the initial mass for Ag, In and Cd, calculated by ASTEC. It can be seen that the burst release of only Cd at the time of rod rupture (see AEKI I13 results), which is probably due to Cd already vaporised in the entire rod (before its rupture), is not reproduced by the code. Indeed, such release is not taken into account in the present modelling of the ASTEC code. However, the total release of Cd is only slightly more than the experimental estimate of mass transported to the sampling point (which may be less than the release itself). Additionally, the Ag release, which occurred mainly during the late phases of the test sequence, and to a lesser extent In release are underestimated. Likely causes are the Ag vapour pressure, for studies are still in progress in order to better determine the evolution of this parameter [3], and the entrainment of liquefied Ag by boiling In or Cd which is not represented.

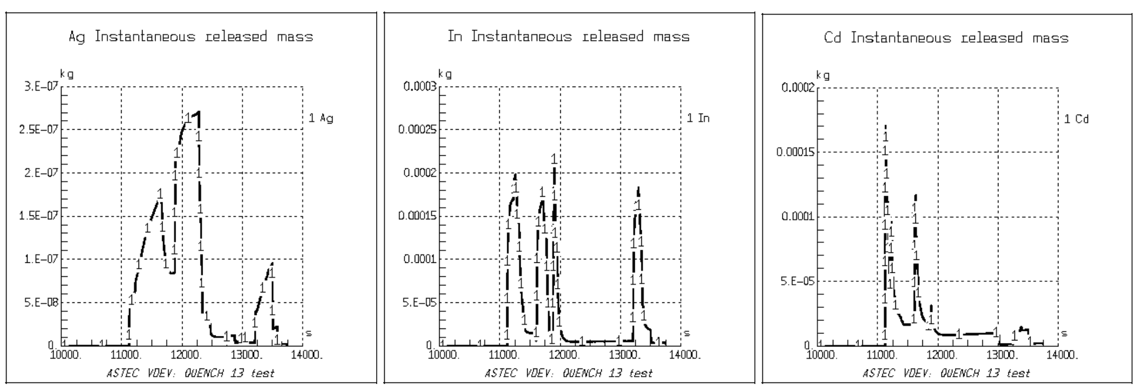

Figure 6: ASTEC calculation of Ag, In, Cd instantaneous released masses

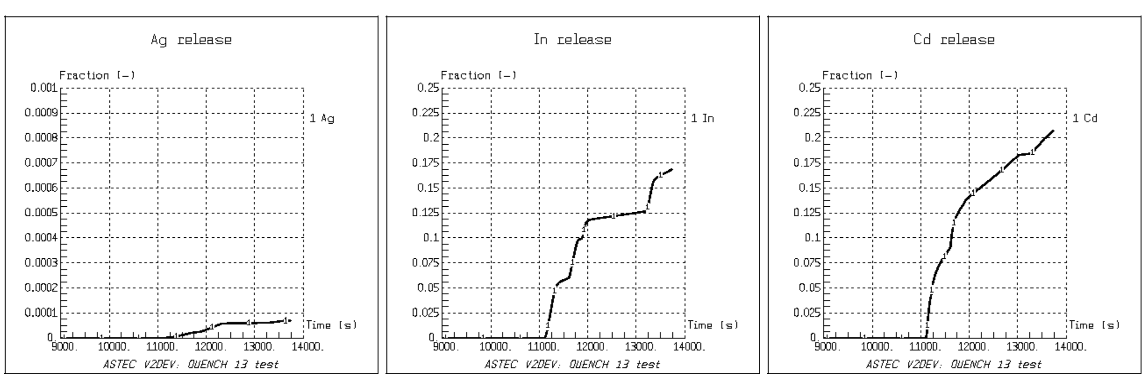

Figure 7: ASTEC calculation of Ag, In, Cd mass fractions

Preliminary post-test calculations with ATHLET-CD showed a rather good agreement concerning the overall thermal behaviour, although hydrogen generation was slightly underestimated. About 150 g of absorber material were calculated to melt and relocate. The results, shown in figure 8, confirm experimental findings concerning Cd burst release and are comparable with the estimated total. As in the pre-test calculations [7] and the ASTEC results (see figure7), ATHLET calculates only a rather small Ag release. However, further in-depth analyses are planned as soon as the direct experimental analysis is complete.

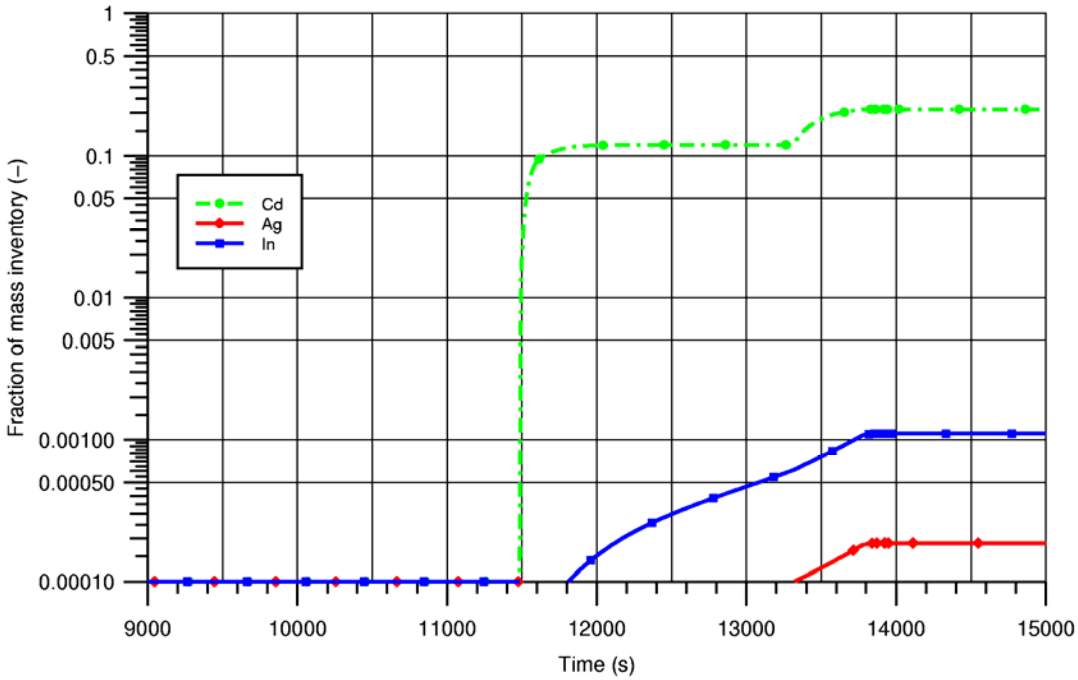

Figure 8: ATHLET-CD calculation of integral Ag-In-Cd release

The MAAP4 code has been used at EDF R&D to simulate the QUENCH-13 experiment. The initial MAAP modelling shows large aerosol releases: cadmium is estimated to be fully released, indium at about 50 % and silver at about 5 % (fig 9: in black). The kinetics of cadmium and indium releases are obviously too fast. Improvements of the MAAP model have been implemented. The control rod rupture is now considered in the current node instead of the whole rod. This strongly reduces the calculated releases of cadmium and indium. Besides, eutectics interaction between molten SIC and zirconium of the guide tube is introduced in the model. Previous experiments showed liquefaction of Zr interacting with molten SIC between 1200 and 1400 °C; this change of phase is modelled, starting at 1200°C and complete at 1400°C. This modelling has only a small impact on the calculated releases. Results of the new model are shown on figure 9 (in red). The calculated Cd and In releases are respectively around 8 and 4 % while the Ag release is now at 2.5%. Such results are in better accordance with the test findings. MAAP uses vapour pressures at equilibrium to calculate releases. Silver partial pressure exceeds 1 mbar over around 1300°C, so early release is possible. Silver vapour arriving in a cooler zone forms aerosols which are driven by the bulk flow, but are not deposited in the core in the MAAP model. The somewhat large release (greater than Cd-In) may seem to be an overestimate, considering the analysed samples, but silver may have deposited before the measurement point. The samples which contained Ag included comparatively large particles, and may have been deposited more than Cd and In. Finally, table 5 compares the calculated releases with the estimates of SIC transported past the on-line measurement location, expressed as percentage of initial inventory.

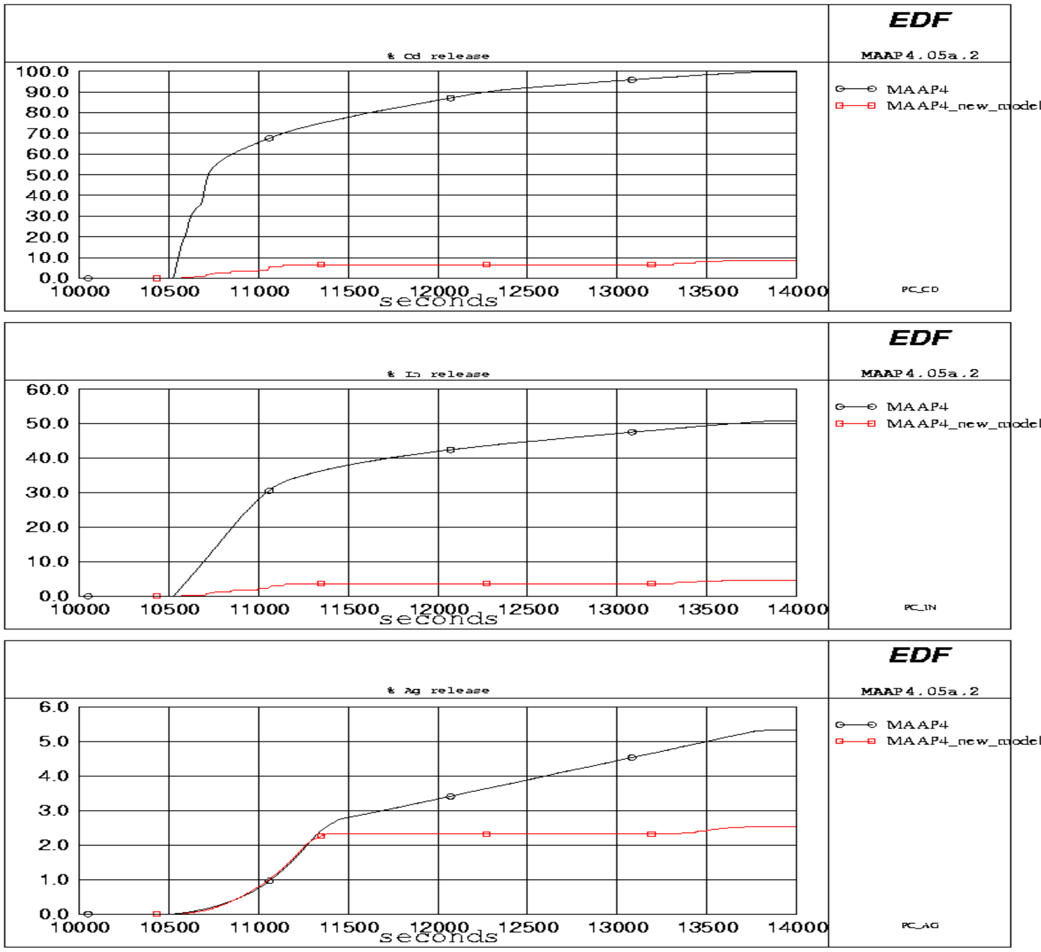

Figure 9: MAAP calculation of Cd, In and Ag releases from the bundle

	Ag	In	Cd
ASTEC *	0.008	17	21
ATHLET-CD *	0.02	0.11	21
MAAP-4 (revised) *	2.5	4.5	8.5
Experimental estimate	0.5 – 2.5	1.5 - 4	10 - 20

Table 5: Comparison of SIC release fractions (* released; ** transported)

4. CONCLUSIONS

QUENCH-13 was successfully conducted at FZK following detailed, coordinated planning analyses by PSI, GRS and EDF, as well as complementary separate effects test on short control rod samples.

The test results are providing important information on the impact of control rod failure on the release of SIC and its impact on bundle degradation and on aerosol transport in an integral transient sequence. Post-test examinations are still in progress.

The occurrence of control rod failure at temperatures well below the melting point of steel was conformed for the representative geometry and conditions of QUENCH-13

The detailed bundle examinations are not complete, and it is not yet clear whether molten SIC interacted strongly with cladding from the nearby heater rods. There is indirect evidence from the local reduction in temperatures and oxidation rate that impingement of SIC on nearby rods affected the character of the cladding in some way.

Analyses using a variety of system-level and detailed codes enabled a preliminary assessment of the respective modelling capability. The following trends are indicated:

(i) All of the models provided adequate treatment of the thermal-hydraulic sequence up to control rod failure, a pre-requisite for interpretation of the degradation and aerosol transport processes and assessment of the respective models.

(ii) The processes associated with release and relocation of molten SIC impose a strong challenge to the code models. Further analyses are necessary before a clear statement can be made concerning bundle thermal-hydraulic response after control rod failure.

(iii) SCDAP is the only code used which includes a kinetic model, albeit idealised, for the control rod failure. Although the code reproduced quite well the observed failure temperature, data from other tests indicate that the interaction processes are more complicated and that a degree of basic uncertainty remains.

(iv) ASTEC, ATHLET and MAAP gave credible accounts of the Cd and In, release, but only MAAP calculated significant release of Ag. Quantitatively, the models showed wide scatter in release fraction and rates; assessment and improvement should continue.

(v) The code models should include material interactions between SIC, stainless steel and Zircaloy. Results of a recently modified version of MAAP indicate that SIC interactions with other materials may influence the release of SIC aerosols.

(vi) The pre-and post test analyses demonstrate the value of coordinated effort using a variety of modelling tools.

The QUENCH-13 experiment will be valuable to qualify improvements in the code models, especially in phenomena involving the SIC control rod. Analyses will continue when all the experimental data are available.

REFRENCES

[1] D.A. Petti, “Silver-Indium-Cadmium Control Rod Behaviour and Aerosol Formation in Severe Reactor Accidents”, NUREG/CR–4876, April 1987.

[2] D.A. Petti, “Silver-Indium-Cadmium Control Rod Behaviour in Severe Reactor Accident”, Nucl. Technol. **84**, 128 (1989).

[3] R. Dubourg et al., “Understanding the Behaviour of Absorber Elements in Silver-Indium-Cadmium Control Rods during PWR Severe Accident Sequences”, Proc. ERMSAR 2008, Paper 2.6, Nesseber, Bulgaria, 23-25 September 2008.

[4] L. Sepold et al., “AgInCd Absorber Test QUENCH-13: Quick Look Report”, FZK Report NUKLEAR 3416 (2008).

[5] J. Stuckert. “Some Results of EDX Analysis of Melt and Aerosols Released during the QUENCH-13 Test”, Phebus Meeting, BIC Circle, Bergen, 1-4 March 2008.

[6] M. Steinbrück, M. Große, U. Stegmaier. “Single Rod Experiments on Failure of SIC Control Rods”, Proc. 13th Int. QUENCH Workshop, Karlsruhe, Germany, 20-22 November 2007, ISBN 978-3-923704-63-7

[7] T. Haste et al. “Pre-test Calculation Support for the QUENCH-13 Experiment”, Proc. ICAPP ’08, Paper 8065, Anaheim, Ca., USA, 8-12 June 2008.